Article

The Influence of Alteration of Aggregates on the Quality of the Concrete: A Case Study from Serpentinites and Andesites from Central Macedonia (North Greece)

Petros Petrounias [1],*, Panagiota P. Giannakopoulou [1], Aikaterini Rogkala [1], Panagiotis M. Stamatis [1], Basilios Tsikouras [2] [iD], Dimitrios Papoulis [1], Paraskevi Lampropoulou [1] and Konstantin Hatzipanagiotou [1]

[1] Section of Earth Materials, Department of Geology, University of Patras, 265 04 Patras, Greece; peny_giannakopoulou@windowslive.com (P.P.G.); krogkala@upatras.gr (A.R.); panayiotisstamatis@gmail.com (P.M.S.); papoulis@upatras.gr (D.P.); p.lampropoulou@upatras.gr (P.L.); k.hatzipanagiotou@upatras.gr (K.H.)
[2] Physical and Geological Sciences, Faculty of Science, Universiti Brunei Darussalam, Jalan Tungku Link, Gadong, Bandar Seri Begawan, BE1410 Brunei Darussalam; basilios.tsikouras@ubd.edu.bn
*   Correspondence: Geo.plan@outlook.com

Abstract: This study aims at the interpretation of the adverse effects of the secondary products in two types of rocks during their performance as concrete aggregates. Serpentinised peridotites contain serpentine, as the dominant secondary phase, which creates low microroughness on the particles and therefore unfavorable surfaces for cement paste to adequately adhere to. Moreover, its soft and platy nature contributes to the development of platy defects along the contacts of the aggregate particles with the cement paste. Poor adherence of the paste, failures along the contacts of the aggregate particles and potential propagation of the defects into the concrete during curing (and perhaps subsequently in-service) explain the poor performance of highly serpentinised rocks as concrete aggregates. Andesites show a different composition with a variety of secondary products including albite, chlorite, calcite, Fe-oxides and clay minerals. The role of all these products was investigated and it appears that only smectite is important, as even small amounts of it may be detrimental to the quality of the rocks as concrete aggregates. It is likely that abnormal hydration reactions and considerable swelling of the smectite result in the appearance of defects in the concrete, hence contributing to its low performance.

Keywords: alteration degree; serpentinites; andesites; concrete; aggregates; clay minerals

1. Introduction

Concrete is the most used man-made material and comprises a mixture of mortar, aggregates and water [1–4]. Its fundamental component is a mixture of cement and water, which binds the aggregate particles together [1,5,6]. Usually, aggregate is considered as inert filler, which accounts for 60 to 80% of the volume and 70 to 85% of the weight of concrete. Natural coarse aggregates are various crushed rocks extracted from pits and quarries of different geological sources [7]. The capillary porosity of the aggregate particles is essential for the cohesiveness of the concrete, and thus it is an important factor for the final quality. Igneous rocks have very different capillary pores relative to the majority of sedimentary and metamorphic lithotypes; therefore, they are expected to show dissimilar behaviour [8]. Microstructural characteristics such as microroughness, mineralogical composition,

structure and compressive strength comprise some critical factors for the quality and strength of the concrete [9]. The mineralogical composition of the aggregates and more specifically their degree of alteration strongly influence their mechanical behaviour and in-service performance [10–13]. Increased percentages of certain secondary minerals, such as serpentine and talc, negatively affect the mechanical properties of ultramafic aggregates due to their smooth layers, cleavage and platy or fibrous crystal habit [14,15]. However, other phases, such as quartz or spinel, may improve their strength due to the high hardness and absence of preferred planes of weakness [10,15]. Clay minerals, which are not rare alteration products in volcanic rocks, (e.g., andesites, rhyodacites), show a high capacity to absorb and subsequently lose water, which is accompanied by swelling and shrinkage, respectively [16]. Therefore, the capacity of clay minerals to absorb large amounts of water, preferentially along their eminent cleavage, increases the demand of water in a concrete mix, which in turn may have a detrimental impact on the workability of concrete and hence lead to a weaker and more permeable hardened concrete. Generally, clays are also thought to reduce workability, due to their high surface areas and lamellar structure. Clay minerals have low strength and as a result, if they are present as a coating on aggregates, they might disrupt the paste–aggregate bond. For these reasons, it is of great importance to determine the presence of clay minerals in the aggregates [17–21].

The aim of this study is to investigate how different alteration styles of serpentinites and andesites affect their mechanical properties, as well as how their performance as concrete aggregates is influenced.

2. Geological Setting

The Veria-Naousa ophiolite complex in northern Greece belongs to the Almopias subzone of the Axios geotectonic zone (Figure 1). It consists, from base to top, of serpentinised lherzolite and harzburgite, which are cut by scarce pyroxenite dykes, gabbro, diabase and pillow basalt [22]. Small bodies of pyroxenites occur within the serpentinised harzburgite, as well. This sequence is considered to be a remnant oceanic lithosphere, which has been emplaced onto Late Triassic–Jurassic platform carbonates of the Pelagonian Zone, during Upper Jurassic to Lower Cretaceous [23–29]. Serpentinised peridotites are least to moderately weathered and highly affected by tectonic processes, expressed by an intense network of joints. Rare rodingite dykes occur in these ultramafic rocks. Conglomeratic limestone, flysch and breccia limestone of Neogene to Quaternary age lie uncomfortably on the ophiolitic rocks. Granite to granodiorite intrusion is observed near Trilofos village. The eastern contact of the ophiolite with the Pelagonian carbonates is dominated by a cataclastic zone comprising diabasic fragments cemented with numerous random albitite veins. Pliocene volcanic rocks of the Almopias subzone, ranging in composition from trachyte to andesite with variable degrees of weathering, occur to the east of the ophiolitic complex. Nd/Sr isotopic data indicate that they are associated with melting of the mantle wedge in a supra-subduction zone regime [30].
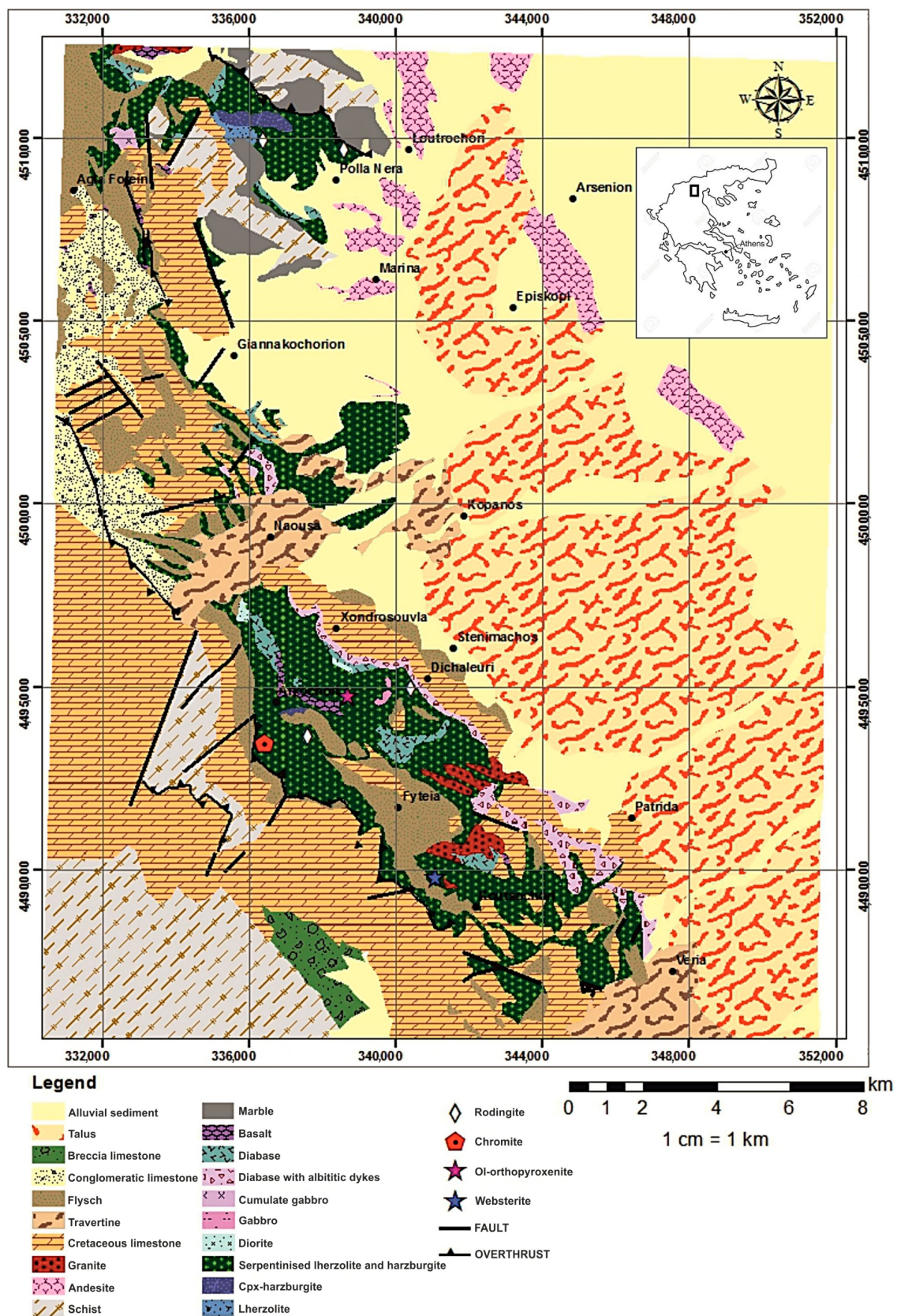
Figure 1. Geological map of the Veroia sheet IGME [31] (modified after fieldwork and mapping by using ArcMap 10.1); black rectangle in the inset shows the study area.

3. Materials and Methods

3.1. Materials

Crushed aggregates from two different lithological types (serpentinites and andesites), which showed least weathering, from the Veria-Naousa region in central Macedonia were tested. Seven concrete specimens were prepared and tested from the same aggregates, using normal Portland cement (CEM II 32.5N), which is conformed to EN 197-1 [32]. Potable tap water, free of impurities such as salt, silt, clay and organic matter, with pH = 7.0, was used for mixing and curing the concrete. In order to keep a consistent composition for all the concrete specimens, we adopted the principle of maintaining the same volume of aggregate per m^3 of the mixture. The proportions of the concrete mixtures, by mass, were 1/6/0.63 cement, aggregate and water ratio.

3.2. Methods

3.2.1. Test Methods for Aggregates

The resistance to fragmentation of the crushed aggregates was tested using the Los Angeles (LA) abrasion machine, according to the LST EN 1097-2:2001 [33]. Uniaxial compressive strength (UCS) of the rock samples was examined on core cylindrical samples, according to the ASTM D 2938-95 [34] specification and the arithmetic mean value from six specimens of each sample was calculated.

The mineralogical and microtextural characteristics were examined in polished-thin sections with a polarising microscope, according to EN-932-3 [35] standard for petrographic description of aggregates. The bulk samples as well as their clay fractions (<2 μm) of the investigated samples were determined by powder X-ray diffraction (XRD), using a Bruker D8 Advance Diffractometer (Bruker, Billerica, MA, USA), with Ni-filtered CuK_α radiation. The <2 μm clay fraction was separated by settling and dried on glass slides at room temperature. Random powder mounts were prepared by gently pressing the powder into the cavity holder. The scanning area for bulk mineralogy of the specimens covered the 2θ interval 2–70°, with a scanning angle step size of 0.015° and a time step of 0.1 s. For each <2 μm specimen, the clay minerals were scanned from 2° to 30° 2θ and identified from three XRD patterns (after air-drying at 25 °C, ethylene glycol solvation and heating at 490 °C for 2 h). The mineral phases were determined using the DIFFRACplus EVA 12® software (Bruker-AXS, Billerica, MA, USA) based on the ICDD Powder Diffraction File of PDF-2 2006 while the semi-quantitative analyses were performed by TOPAS 3.0® software (TOPAS MC Inc., Oakland, CA, USA), based on the Rietveld method refinement routine. The routine is based on the calculation of a single mineral-phase pattern according to the crystalline structure of the respective mineral, and the refinement of the pattern using a non-linear least squares routine. The quantification errors calculated for each phase according to Bish and Post [18] are estimated to be ~1%, while the detection limit is 2%.

The surface texture of aggregate particles was studied in secondary electron images (SEI) according to BS 812 Part 1 [36], which outlines six qualitative categories: glassy, smooth, granular, rough, crystalline, honeycomb and porous.

3.2.2. Test Methods for Concrete

Seven normal concrete cube specimens (150 mm × 150 mm) were prepared from the two different aggregate types, according to ACI-211.1-91 [37]. All parameters (aggregate size and ratios of water, cement and commercial carbonate sand) remained constant in all the concrete specimens. The aggregates were crushed and sieved through standard sieves and separated into the size classes of 2.00–4.75, 4.45–9.5, and 9.5–19.1 mm.

After 24h, the samples were removed from the mold and were cured in water for 28 days. Curing temperature was 20 ± 3 °C. These specimens were tested in a compression testing machine at an increasing rate of load of 140 kg/cm^2 per minute. The compressive strength of concrete is calculated by the division of the value of the load at the moment of failure over the area of specimen. The compression test was elaborated according to BS EN 12390-3:2009 [38].

After the compressive strength test, the textural characteristics of concretes were examined. Polished-thin sections were studied in a polarising microscope according to ASTM C856–17 [39].

4. Test Results

4.1. Mechanical Properties of Aggregates

UCS and LA values of the tested rocks display a wide variation even within the same lithology. UCS in the serpentinites ranges from 34.00 to 76.00 MPa showing a broad overlap with these values in the andesites ranging between 35.62 and 53.00 MPa (Table 1). The serpentinites and andesites show different LA values, which however are rather high in both rock-types. The serpentinites are less resistant with LA values ranging from 17.00% to 25.51%, whereas the andesites show LA values between 18.36% and 35.00% (Table 1).

Table 1. Results of mechanical properties of the studied aggregates (each uniaxial compressive strength (UCS) value is the mean from six samples).

Samples	Lithotypes	Uniaxial Compressive Strength of Rocks (UCS MPa)	Los Angeles (LA %)
BE.82	Andesite	35.62	35.00
BE.88	Andesite	53.00	18.36
BE.89	Andesite	45.00	23.98
BE.01	Serpentinite	76.00	17.00
BE.12	Serpentinite	55.40	23.00
BE.103	Serpentinite	34.00	25.51
BE.133	Serpentinite	35.00	22.50

4.2. Petrographic Features of Aggregates

4.2.1. Serpentinites

The serpentinites show mainly a cataclastic texture (Figure 2), due to intense brittle deformation and a variety of secondary textural features. Their primary modal mineralogical composition is less than 30% and includes relics of orthopyroxene, Cr-spinel, as well as rare olivine and scarce clinopyroxene (Figure 2a,b). Orthopyroxene appears as subhedral porphyroclasts and most of them show exsolution lamellae of clinopyroxene, typical feature of upper mantle peridotites. Serpentine is the major secondary phase showing primarily typical mesh, as well as local bastite after orthopyroxene and ribbon textures (Figure 2c). Chlorite and magnetite are also products of hydrothermal alteration of these peridotites. Magnetite commonly fills microcracks or rims of Cr-spinel crystals. Brittle deformation is expressed mainly by intense fragmentation of spinel, as well as by intergranular microcracks (Figure 2d).
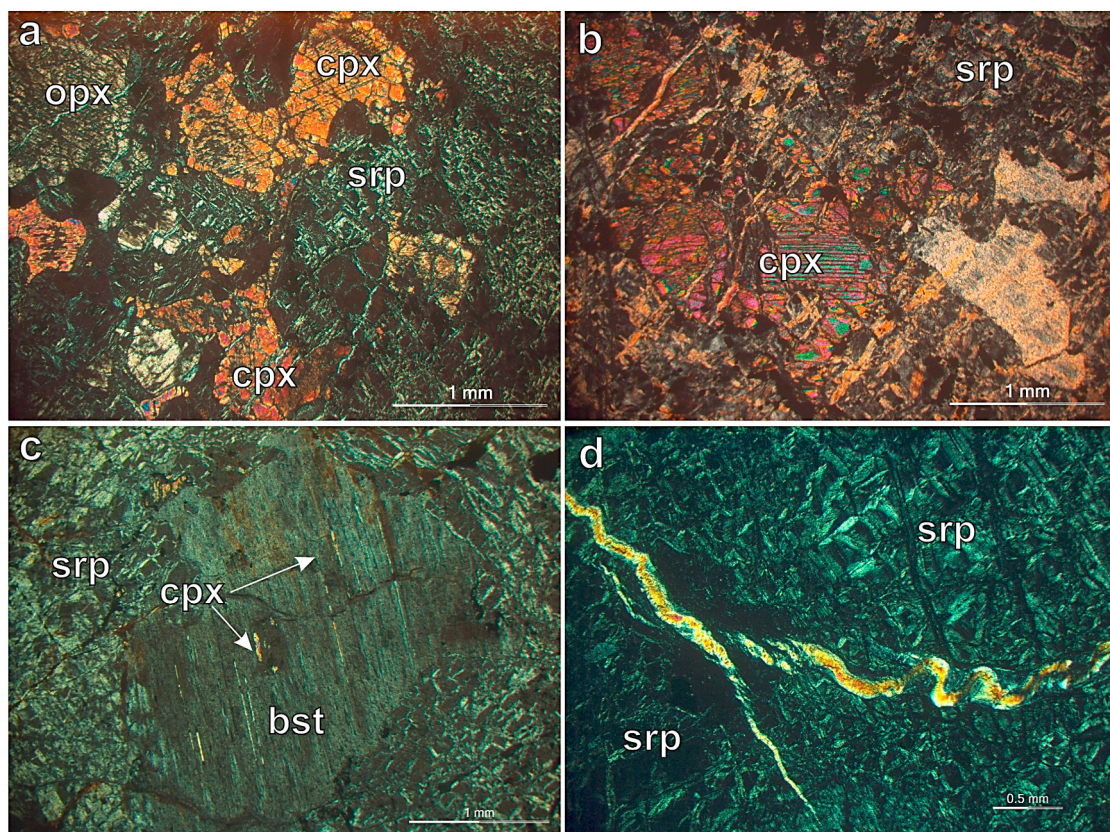
Figure 2. Photomicrographs of serpentinites showing (**a**), (**b**) relics of orthopyroxene and clinopyroxene in serpentinised matrix (sample BE.01, XPL); (**c**) bastite orthopyroxene porphyroclast with exsolution lamellae of clinopyroxene (sample BE.133, XPL); (**d**) mesh texture of serpentinised matrix with intragranular microcracks partially filled with serpentine as well (sample BE.103, XPL). Abbreviations: opx: orthopyroxene, cpx: clinopyroxene, srp: serpentine, bst: bastite.

4.2.2. Andesites

The collected andesite samples are vesicular and have a porphyritic texture with phenocrysts of plagioclase (up to 0.8 mm), K-feldspar, biotite and lesser clinopyroxene surrounded by a microcrystalline and amorphous groundmass (Figure 3a,b,c). In places, flow structures can be observed. Local plagioclase phenocrysts are rimmed by sanidine. Plagioclase phenocrysts are optically zoned showing both normal and oscillatory reverse zoning (Figure 3d). Accessory minerals commonly include apatite, titanite, zircon and magnetite. Alteration products in the andesites include clay minerals, albite, chlorite, Fe-oxides and calcite (Figure 3c,d). Numerous intragranular cracks are present as a result of brittle deformation.

4.3. X-ray Diffractometry of Aggregates

The X-ray diffraction enabled us to identify the crystalline phases of the studied rocks. Representative XRD patterns of the samples are shown below (Figure 4).
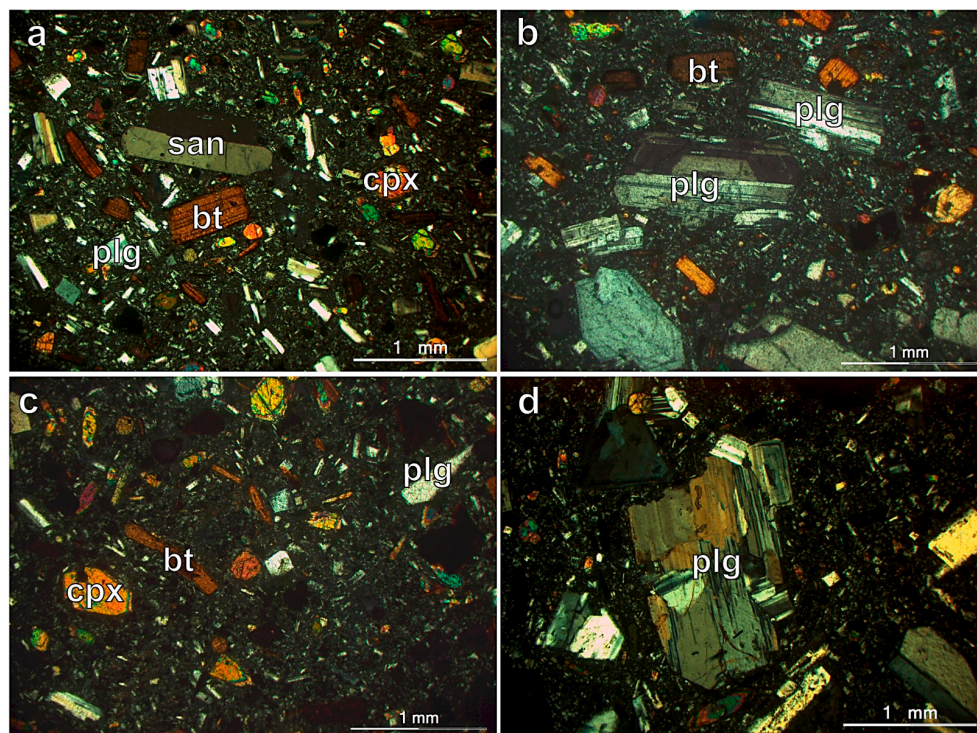
Figure 3. Photomicrographs of andesites: (**a**) porphyritic texture with plagioclase, K-feldspar (sanidine), clinopyroxene and biotite phenocrysts (sample BE.89, XPL); (**b**) porphyritic texture with plagioclase and biotite phenocrysts; (**c**) phenocrysts of oxidised biotite, clinopyroxene and zoned plagioclase in a microcrystalline to glassy groundmass (sample BE.88, XPL); (**d**) phenocryst of a zoned and altered to albite plagioclase surrounded by glassy groundmass (sample BE.82, XPL). Abbreviations: plg: plagioclase, san: sanidine, cpx: clinopyroxene, bt: biotite.
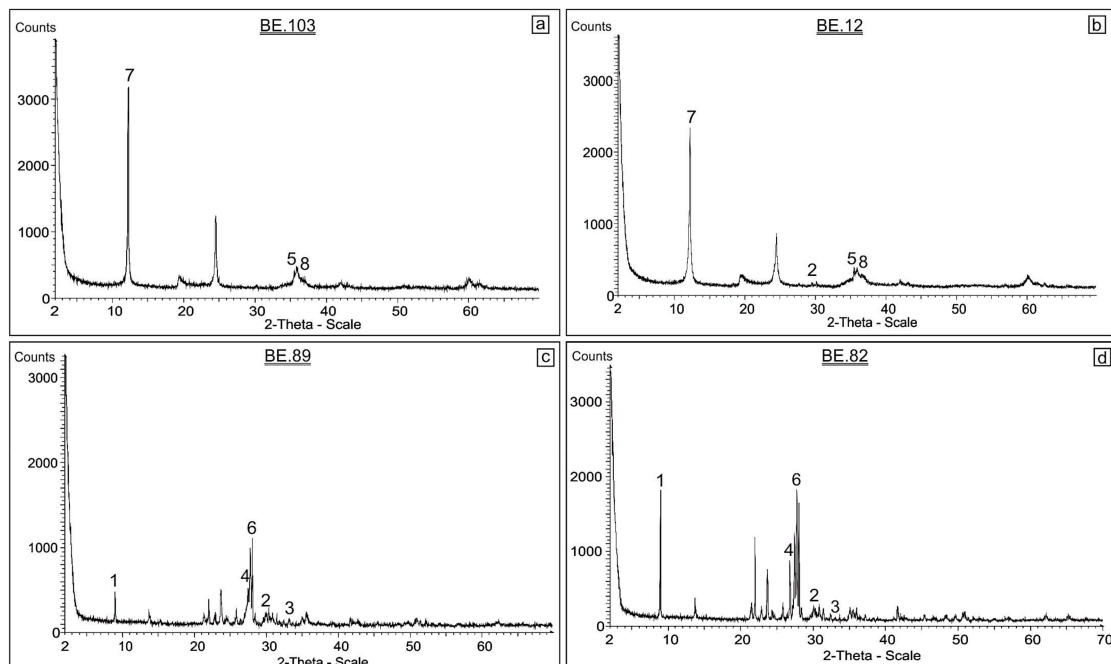

Figure 4. Representative X-ray diffraction patterns of the studied serpentinites (**a**, **b**) and andesites (**c**, **d**). Sample numbers are indicated as insets (1: mica, 2: diopside, 3: hematite, 4: K-feldspar, 5: magnetite, 6: plagioclase, 7: serpentine, 8: spinel).

In this case study, for the accurate identification of the type of clay minerals (contained in the studied andesite samples), the samples were size fractionated and studied after ethylene-glycol and thermal treatment (Figure 5).

Bulk composition and clay minerals from the clay fraction were quantified using the Rietveld method (Table 2). The obtained compositions are consistent with our petrographic observations under the polarising microscope.

Study of XRD patterns revealed the presence of illite in sample BE.88 and the presence of both illite and smectite-group minerals in samples BE.82 and BE.89.
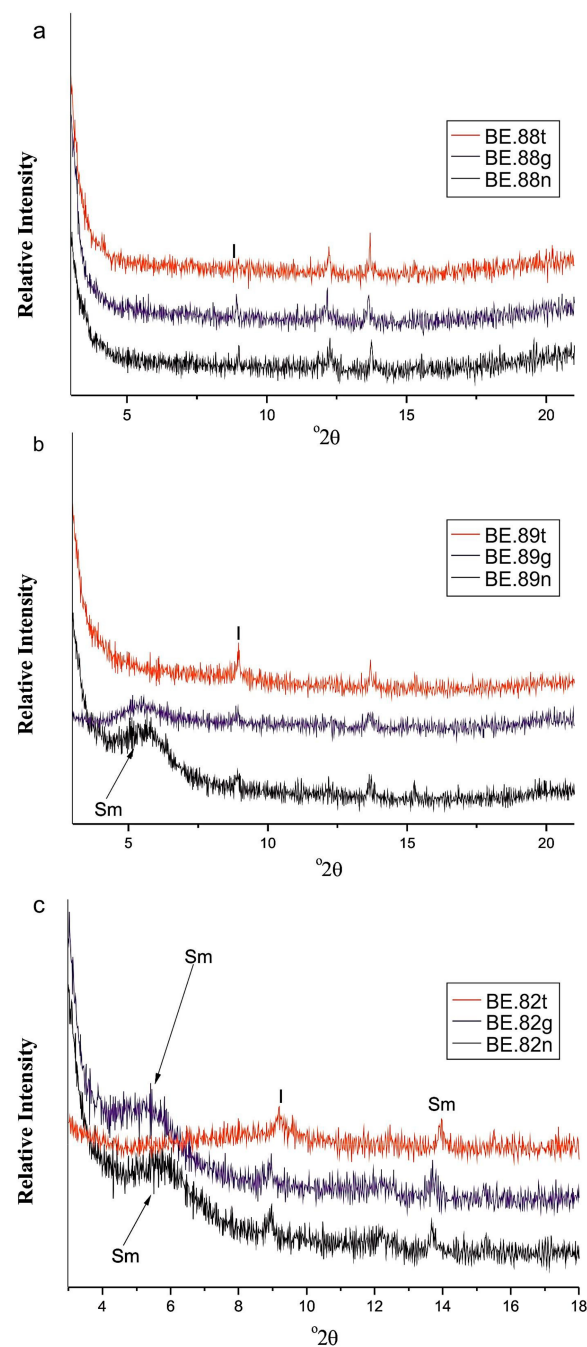

Figure 5. X-ray diffraction patterns of the clay fraction from three andesite samples: (**a**) sample BE.88; (**b**) sample BE.89; (**c**) sample BE.82. Sample numbers are given in the insets (n: air dried, g: glycolated, t: heated, Sm: smectite, I: Illite).

Table 2. Mineralogical composition of the studied rocks from XRD analysis (-: not detected). Quantification errors of ~1% are calculated for each phase according to Bish and Post [18].

Samples	BE.82	BE.88	BE.89	BE.01	BE.12	BE.103	BE.133
Spinel	-	-	-	10.0	9.6	6.5	1.5
Orthopyroxene	-	-	-	8.0	-	-	3.6
Clinopyroxene	7.6	9.0	8.7	7.7	-	5.1	2.1
Serpentine	-	-	-	70.7	85.4	87.0	91.4
Magnetite	-	-	-	4.3	5.0	1.4	1.5
Hematite	2.0	0.6	1.0	-	-	-	-
K-feldspar	25.2	29.1	25.1	-	-	-	-
Plagioclase	52.8	45.8	55.1	-	-	-	-
Biotite	5.6	7.2	6.1	-	-	-	-
Illite	3.8	8.3	3.1	-	-	-	-
Smectite	2.8	-	0.9	-	-	-	-

4.4. Surface Texture of Aggregates

The surface textures of aggregate particles were studied with the aid of secondary electron images (SEI). Differences in microroughness are apparent between the serpentinites and the andesites. Sample BE.133 is nearly completely serpentinised resulting in a smooth and vitreous surface texture (Figure 6a). With decreasing alteration (i.e. decreasing contents of serpentine; see Table 2) the surface of the particles appears rough (Figure 6b). This is explained by the platy and soft tendency of serpentine. The surface textures of the andesite particles are independent of their degree of alteration. All samples display rough surfaces, which are assigned to the presence of various phenocrysts (feldspars, biotites) with variable hardness and much different habits (and hardness) than their host glassy and brittle groundmass (Figure 6c,d).
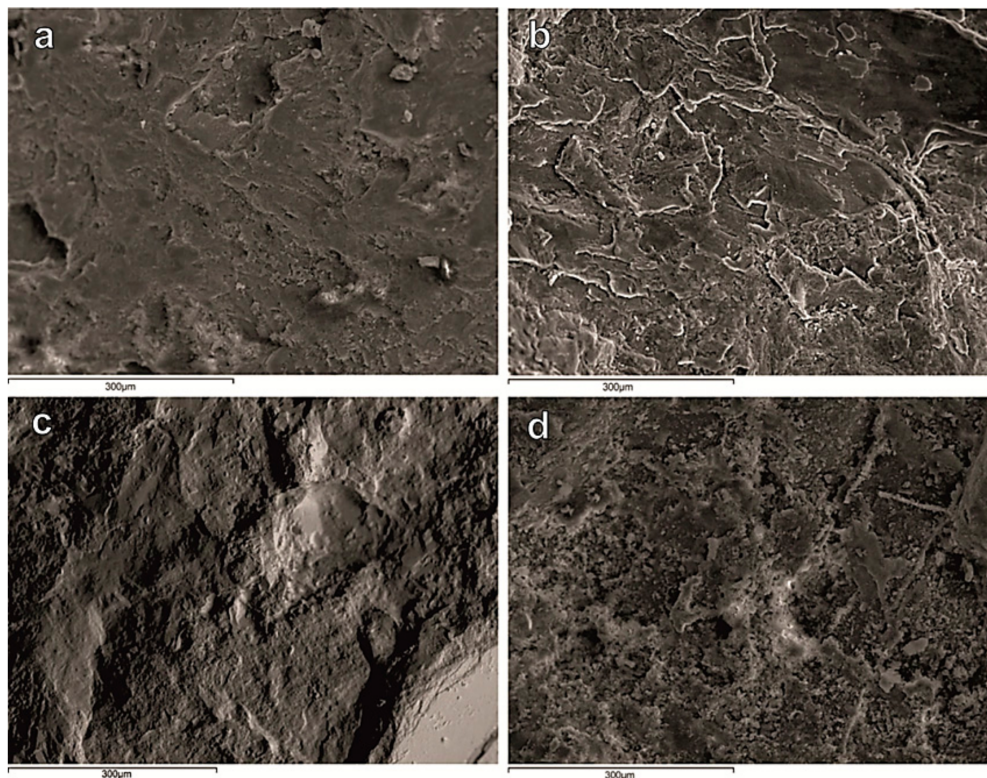

Figure 6. Back scattered electron images showing the surface texture from representative serpentinites (**a**: sample BE.133 and **b**: sample BE.103) and andesites (**c**: sample BE.82 and **d**: sample BE.89).
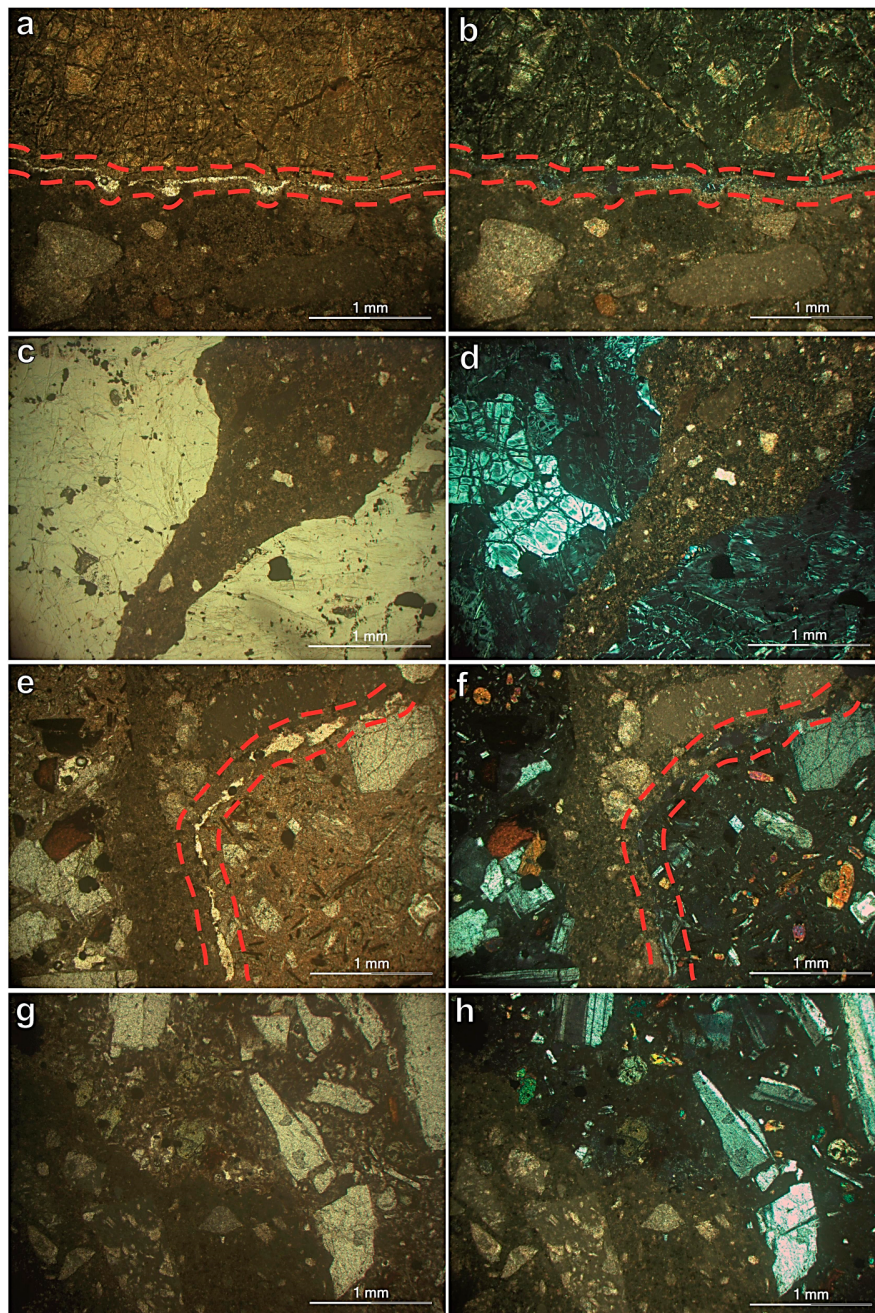
Figure 7. Photomicrographs of representative tested concretes: (**a**), (**b**) bad cohesion between the cement paste and the serpentinite aggregate particle (sample BE.103, PPL, XPL); (**c**), (**d**) good cohesion between the cement paste and the serpentinite aggregate particle (sample BE.01, PPL, XPL); (**e**), (**f**) bad cohesion between the cement paste and the andesite aggregate particle (sample BE.82, PPL, XPL); (**g**), (**h**) good cohesion between the cement paste and the andesite aggregate particle (sample BE.88, PPL, XPL). Red lines constrain the contacts between aggregate particles and cement paste.

4.5. Test Results for Concrete

Results from the concrete testing are listed in Table 3. The concrete specimens prepared with both serpentine and andesite aggregates do not show significant differences in their UCS values. Failure of the specimens made with the serpentinites range at stress from 25.00 to 30.00 MPa whereas those prepared with andesites show slightly lower strengths (but with a large overlap) at 23.00 to 27.33 MPa. The concrete specimen BE.01 was prepared with the least serpentinised aggregates.

Table 3. Compressive strength of concrete specimens prepared with serpentinites and andesites

Sample No.	BE.82	BE.88	BE.89	BE.01	BE.12	BE.103	BE.133
Aggregate type		Andesites			Serpentinites		
Concrete UCS (MPa)	23.00	27.33	25.00	30.00	26.00	26.00	25.00

The tested concrete specimens were subsequently examined under polarising and scanning electron microscopes for the degree of cement hydration, microcracking and potential reaction products. Careful observation of the polished-thin sections revealed variable characteristics for the cohesion between the cement paste and the aggregate particles for both the serpentinites and andesites. Some places show microcracks (presumably developed after concrete UCS) along the interfaces between the cement paste and the aggregate particles, which are assigned to de-bonding while some others show good cohesion between the aggregate particles and the cement paste (Figure 7).

Scanning electron microscopy was employed to elaborate the reasons for this variable behaviour. Backscattered electron images show that only biotite phenocrysts, from the andesitic aggregates, are strongly associated with the appearance of zones of weakness (Figure 8a,b). Thus, the observed de-bonding is related to zones of higher concentrations of biotite, as the accumulation of weak zones have a profound effect on the cohesion of the concrete. A reaction zone of few microns thick is locally observed between the cement paste and serpentinite aggregates (Figure 8c,d). Moreover, the serpentinite aggregate particles show platy separation surfaces, presumably controlled by the eminent cleavage of serpentine (Figure 8c). Both these phenomena are proportional to the serpentine contents, as they are more frequent in the more serpentised samples and they are considered as the principal factor of de-bonding of the aggregates from the cement paste.
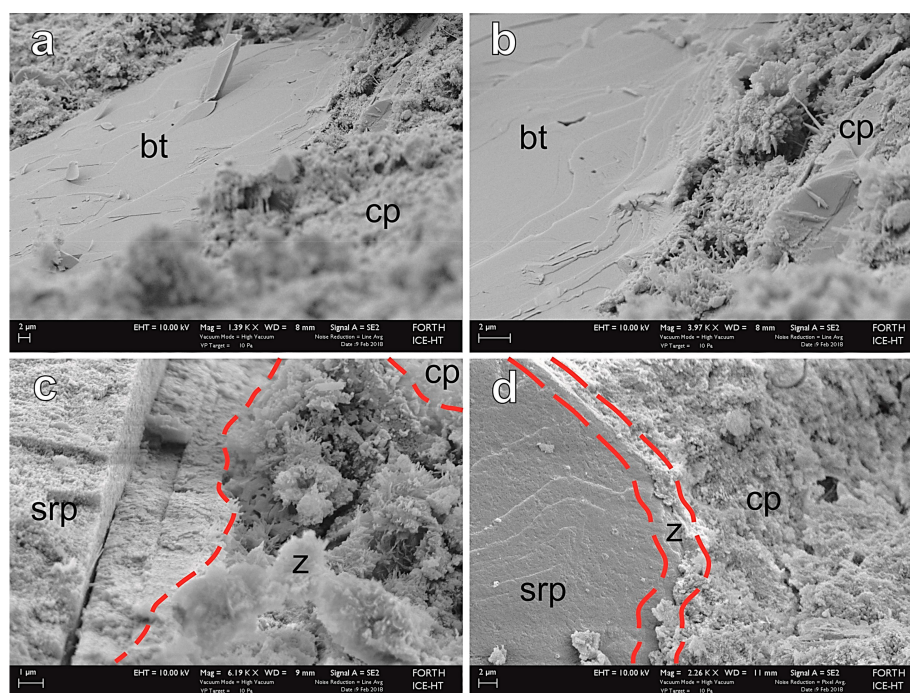

Figure 8. Back-scattered electron images of concrete specimens: (**a**), (**b**) large phenocrysts of biotite create surfaces of weakness in a concrete specimen made with andesite aggregates (sample BE.82); (**c**) formation of a reaction zone and abrupt platy separation between a serpentinite particle and the cement paste in concrete specimen BE.133; (**d**) reaction zone between a serpentinite particle and the cement paste in concrete specimen BE.103. Abbreviations: bt: biotite, cp: cement paste, srp: serpentinite aggregate, z: reaction zone. Red lines constrain reaction zones formed between aggregate particles and cement paste.

5. Discussion

5.1. The Influence of Serpentinisation in the Performance of the Serpentinites

Mineralogical composition, textural features, degree of alteration/deformation and weathering are the main factors affecting the physico-mechanical properties of rock aggregates and consequently their suitability in industrial applications [40–42].

Serpentinisation is an important geochemical process accompanying the formation of the ocean floor [43]. During this process, anhedral or squat crystals of olivine and pyroxene transform to serpentine, a laminate, soft mineral, which belongs to the phyllosilicate subclass of minerals and forms smooth surfaces [44,45]. The influence of serpentine on the mechanical properties of aggregates has been investigated by several researchers [10,14,15,40] who reported UCS and LA ranges from serpentinised peridotites and andesites similar to those documented in the present study. The commonest statistical method used for the determination of the correlations between the various engineering parameters of rocks is regression analysis [46]. In this case study, it appears that the increase of serpentine percentage in the studied serpentinites is accompanied by a simultaneous linear decrease of their UCS (Figure 9a). Moreover, with increasing serpentine contents, their ability in the resistance of abrasion, attrition and grinding is reduced, as is expressed by the increasing LA values (Figure 9b). This trend can be explained from the increased quantities of the soft and platy (or fibrous) serpentine grains, which also show an eminent cleavage, which contribute to the development of abundant zones of weakness. Regression analysis shows strong correlations between the mechanical properties of the aggregates (UCS and LA) and their abundance in serpentine (Figure 9a,b). The validity of these correlations was tested with the aid of t-test and probability figure (p-value). In spite of the small sample population, the absolute value of the t-test for the correlation of the serpentine contents in the rocks with their LA values is much higher than the critical t-table value, for a typical confidence level of 95% and even for higher confidence levels (Table 4). The statistically significant correlation between the LA and the serpentine contents is further substantiated by the very low p-value for the same pair. The correlation of the serpentine contents in the rocks with their UCS values is weaker, as the relevant t-test value is smaller than the critical t-table value, for a confidence level of 95%, and the p-value is relatively higher than the arbitrary limit of p = 0.05 (Table 4). However, we can reject the null hypothesis and consider the correlation valid, if we lower the confidence level at 90% (Table 4). Strong correlations between serpentine contents and LA values in rocks are not unusual and have been reported from other studies (e.g., [15]).

Unlike samples BE.103 and BE.133, which are highly serpentinised, sample BE.01 includes more relics of spinel, olivine and orthopyroxene crystals, which are rather uniformly distributed in the sample, as a result of its mesh texture. The preservation of a rough surface in this sample is attributed to the coexistence of these hard minerals with the soft serpentine, as well as to the more or less even distribution of them, due to the mesh texture. The concrete samples, which were prepared with less serpentinised aggregates, show a good cohesion under microscopic observation, unlike those which were prepared with highly serpentinised aggregates that contain numerous cracks and de-bondings between the aggregate particles and the cement paste. Presumably, the microroughness of the aggregate particles plays a very important role in the adherence of the cement paste. The high microroughness of the aggregate particles, which is related to the presence of less serpentine and to the differential hardness of their minerals, promotes bonding of the aggregates with the cement paste thus leading to higher quality concretes.

5.2. The Influence of Smectites in the Performance of Andesites

The andesite aggregates present variations of their mechanical properties. After searching different varieties, we found out that smectite plays the most important role in the performance of these rocks. Astonishingly, small increases in the presence of smectites cause detrimental effects in the strength and resistance of the andesites. Despite having few samples, clear excellent linear trends can be seen

from the correlation of the smectite abundance in the andesites with their UCS (negative) and LA (positive) values, highlighting the detrimental effects of this mineral on the performance of the host rocks (Figure 9c,d). The statistical significance of these correlations is appraised again using the t-test and the p-value. The significantly higher values of the t-test than the critical t-table, as well as the much lower typical 0.05 p-value of these pairs, for confidence levels even higher than the 95%, strongly suggest the validity of these relationships (Table 4). Illite appears to generally have a negative influence as well, but the correlations of its amounts with the mechanical properties of the andesites are moderate to poor (not shown). Clay minerals belong to the phyllosilicate subclass of the silicate minerals and are natural products of weathering and decomposition of igneous rocks [47]. The smectite group has a 2:1 structure (one octahedral layer sandwiched between two tetrahedral layers) and they have a net charge deficiency. This deficiency is normally balanced by cations (e.g., Na^+, K^+, Ca^{2+}, Mg^{2+} or H^+), which are adsorbed externally on their interlamellar surfaces. The most important smectites include montmorillonite, beidellite, nontronite, saponite and hectorite. The distinguishing characteristic of the smectites is their capacity to absorb water and other polar molecules which subsequently, cause their structure to expand in the direction normal to the basal plane. In this way, the minerals of the smectite group may swell up to 1500% [48] hence causing severe destruction to their host rocks.

Table 4. Paired t-test results for the statistical correlations of the aggregates and the concrete correlations. The listed critical t-table values are for the relevant freedom degrees (dF) and for confidence levels of 99% ($\alpha = 0.01$), 98% ($\alpha = 0.02$), 95% ($\alpha = 0.05$) and 90% ($\alpha = 0.10$).

Pair	T-Test	DF	P-Value	T-Table Values				Figure
				$\alpha = 0.01$	$\alpha = 0.02$	$\alpha = 0.05$	$\alpha = 0.10$	
UCS$_{aggregate}$ - Serpentine	−2.360	3	0.10297	5.841	4.541	3.182	2.353	9a
LA$_{aggregate}$ - Serpentine	−19.790	3	0.00033	5.841	4.541	3.182	2.353	9b
UCS$_{aggregate}$ - Smectite	7.417	2	0.01770	9.925	6.965	4.303	2.920	9c
LA$_{aggregate}$ - Smectite	6.043	2	0.02631	9.925	6.965	4.303	2.920	9d
UCS$_{concrete}$ - UCS$_{aggregate}$	4.282	6	0.00519	3.707	3.143	2.447	1.943	9e
UCS$_{concrete}$ - LA$_{aggregate}$	−0.819	6	0.44431	3.707	3.143	2.447	1.943	9f

5.3. Impact of the Secondary Phases on the Concrete Quality

Textural features, mineralogical composition and degree of alteration of aggregate rocks are important, as they largely influence their performance in various industrial applications including concrete strength [7,9,40–42]. Figure 9e and f illustrate the correlation of the mechanical properties of the concrete specimens against those of their constituent aggregates. Strong, positive, linear correlation of the concrete UCS with the aggregate UCS and a significant, strong, negative, linear correlation of the aggregate LA with the concrete UCS are evident. However, only the first correlation is statistically significant, with the relevant t-test value much higher than the critical t-table value, as well as a very low probability (p-value < 0.05) at a confidence level of 95% and above (Table 4). Very low t-test value and high p-value for the correlation of the LA of the aggregate with the UCS of the concrete does not allow us to reject the null hypothesis. The higher strength of the least serpentinised aggregates apparently resulted in the development of fewer cracks and weak areas, explaining the higher performance of the relevant concrete specimen (Figure 9e). Microscopic observations confirm the fact that the concrete specimen, made with the least serpentinised aggregates, shows fewer defects and imperfections (Figure 7c,d). On the contrary, abundant serpentine in the aggregate particles is considered as a detrimental factor, due to its phyllosilicate habit, which leads to de-bonding from the cement paste under stress. Also, flaws and cracks of highly serpentinised aggregate particles may be activated and expand during curing of the concrete, thus triggering defects and weaknesses in it. Moreover, smooth surfaces of the particles, due to low microroughness, do not favour strong adherence with the cement paste.

　　　Microscopic observation reveals that the concrete specimen made with the smectite-free andesites shows better cohesion than the rest of the specimens (Figure 7g,h). Unlike this, the rest of the samples display extended cracks and detachments along the rims of the aggregate particles with the cement paste (Figure 7e,f). This is consistent with the fact that the concrete with the smectite-free andesite aggregates shows the highest UCS (Figure 9e). The andesite particles show high microroughness, unlike the serpentinite ones, therefore the presence of clay minerals in them does not affect this factor and it cannot be a reason for the observed inadequate cohesiveness. A likely interpretation for this behaviour is the fact that water absorbance and swelling of smectites resulted in abnormal hydration reactions between the cement paste and the aggregate particles, as well as stress increase and hence instability after the concrete curing. Concrete fine aggregates with smectite, present significant losses of slump, increased water requirements and potential drying shrinkage volume changes due to the presents of this clay mineral [49]. On the other hand, kaolinite and illite are both non-swelling. These differences in the swelling characteristics of different clays are related to their chemical composition and structure [50]. Insignificant negative impacts of illite and kaolinite on the quality of the host rock and the concrete are confirmed from this study. However, small amounts of smectite play an adverse role in the quality of their host rock, as well as in the quality of the concrete specimens, which are prepared with them.
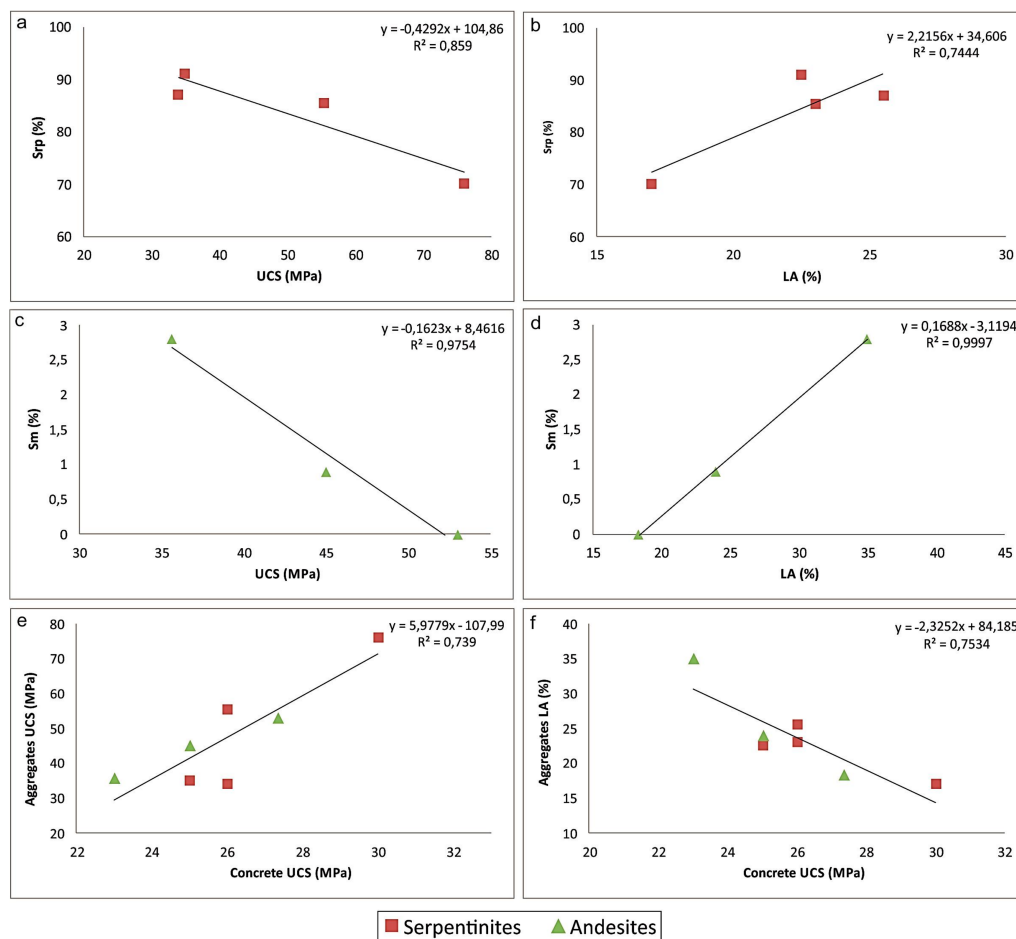

Figure 9. Serpentine abundance (srp) in the serpentinite aggregates plotted against their uniaxial compressive strength (**a**) and their Los Angeles values (**b**); smectite abundance in the andesite aggregates plotted against their uniaxial compressive strength (**c**) and their Los Angeles values (**d**); uniaxial compressive strength of the concrete specimens plotted against uniaxial compressive strength (**e**) and Los Angeles values (**f**) of their aggregates.

6. Conclusions

The secondary products of serpentinites and andesites largely influence their mechanical properties, which definitely have an adverse effect on their performance as concrete aggregates. Increasing serpentine contents result in weaker and less resistant host rocks, as well as to the development of low to negligible microroughness of the aggregate particles. Subsequently, these features have a negative influence on their quality as concrete aggregates. Initial planes and zones of weakness, largely controlled from the excellent cleavage of the soft serpentine, are likely activated during curing (and apparently later in-service) and may expand in the concrete triggering flaws and cracks, thus lowering its quality. Less serpentinised rocks show better performance and moreover the differential hardness of the juxtaposed hard olivine, pyroxene and spinel (primary relics) with the soft serpentine promotes surface roughness, thus resulting in better adherence of the aggregate particles with the cement paste and better quality of concrete.

The existence of smectites in the andesites is detrimental, as even small amounts may cause severe damage. It is likely that smectites from the alteration of felsic minerals adsorb water during the preparation of concrete. Despite the fact that the aggregates always maintain a high microroughness, abnormal hydration reactions and the subsequent swelling of the smectites exert stress and cause defects and de-bonding between the aggregate particles and the cement paste. The combination of the petrographic analysis provides a useful tool for the selection of rocks suitable for the concrete production.

Author Contributions: Petros Petrounias participated in the fieldwork, the elaboration of laboratory tests, the interpretation of the results, coordinated the research and wrote the paper; Panagiota P. Giannakopoulou participated in the interpretation of the results and wrote the paper; Aikaterini Rogkala participated in the fieldwork and performed the SEM work; Panagiotis M. Stamatis participated in the elaboration of the laboratory tests and the interpretation of the results; Basilios Tsikouras participated in the fieldwork, in the interpretation of the results and in writing the paper; Dimitrios Papoulis participated in the elaboration of the mineralogical analyses of clay minerals and in the interpretation of the results; Paraskevi Lampropoulou carried out the XRD analyses; and Konstantin Hatzipanagiotou participated in the interpretation of the results.

References

1. Jackson, N. *Civil Engineering Materials*; Macmillan Press Ltd.: London, UK, 1981.
2. LaLonde, W.S.; Janes, M.F. *Concrete Engineering Handbook*; Library of Congress: New York, NY, USA, 1961.
3. *US Concrete Industry Report*; Library of Congress: New York, NY, USA, 2001.
4. Neville, A.M. *Properties of Concrete*, ELSB 5th ed.; Pearson Education Publishing Ltd.: London, UK, 2005.
5. Taylor, G.D. *Materials in Construction*, 2nd ed.; Longman Group Ltd., Longman House: London, UK, 1994.
6. Rajput, R.K. *Engineering Materials*, 3rd ed.; S. Chard & Company Ltd.: Ram Nagar, New Delhi, 2006.
7. Gonilho Pereira, C.; Castro-Gomes, J.; Pereira de Oliveira, L. Influence of natural coarse aggregate size, mineralogy and water content on the permeability of structural concrete. *Constr. Build. Mater.* **2009**, *23*, 602–608. [CrossRef]
8. Piasta, W.; Góra, J.; Turkiewicz, T. Properties and durability of coarse igneous rock aggregates and concretes. *Constr. Build. Mater.* **2016**, *126*, 119–129. [CrossRef]
9. Yilmaz, M.; Tuğrul, A. The effects of different sandstone aggregates on concrete strength. *Constr. Build. Mater.* **2012**, *35*, 294–303. [CrossRef]
10. Rigopoulos, I.; Tsikouras, B.; Pomonis, P.; Hatzipanagiotou, K. The influence of alteration on the engineering properties of dolerites: The example from the Pindos and Vourinos ophiolites (northern Greece). *Int. J. Rock Mech. Min. Sci.* **2010**, *47*, 69–80. [CrossRef]

11. Petrounias, P.; Rogkala, A.; Kalpogiannaki, M.; Tsikouras, B.; Hatzipanagiotou, K. Comparative study of physico-mechanical properties of ultrabasic rocks (Veria-Naousa ophiolite) and andesites from central Macedonia (Greece). *Bull. Geol. Soc. Gr.* **2016**, *50*, 1989–1998.

12. Giannakopoulou, P.P.; Tsikouras, B.; Hatzipanagiotou, K. The interdependence of mechanical properties of ultramafic rocks from Gerania ophiolitic complex. *Bull. Geol. Soc. Gr.* **2016**, *50*, 1829–1837.

13. Yilmaz, N.G.; Goktan, R.M.; Kibici, Y. Relations between some quantitative petrographic characteristics and mechanical strength properties of granitic building stones. *Int. J. Rock Mech. Min. Sci.* **2011**, *48*, 506–513. [CrossRef]

14. Diamantis, K.; Gartzos, E.; Migiros, G. Study on uniaxial compressive strength, point load strength index, dynamic and physical properties of serpentinites from Central Greece: Test results and empirical relations. *Eng. Geol.* **2009**, *108*, 199–207. [CrossRef]

15. Rigopoulos, I.; Tsikouras, B.; Pomonis, P.; Hatzipanagiotou, K. The impact of petrographic characteristics on the engineering properties of ultrabasic rocks from northern and central Greece. *Q. J. Eng. Geol. Hydrogeol.* **2012**, *45*, 423–433. [CrossRef]

16. Tiwari, B.; Ajmera, B. Consolidation and swelling behavior of major clay minerals and mixtures. *Appl. Clay Sci.* **2011**, *54*, 264–273. [CrossRef]

17. Bish, D.L.; Howard, S.A. Quantitative phase analysis using the Rietveld Method. *J. Appl. Cryst.* **1988**, *21*, 86–91. [CrossRef]

18. Bish, D.L.; Post, J.E. Quantitative mineralogical analysis using the Rietveld full pattern fitting method. *Am. Mineral.* **1993**, *78*, 932–940.

19. McCusker, L.B.; Von Dreele, R.B.; Cox, D.E.; Louer, D.; Scardi, P. Rietveld refinement guidelines. *J. Appl. Crystallogr.* **1999**, *32*, 36–50. [CrossRef]

20. Hillier, S. Accurate quantitative analysis of clay and other minerals in sandstones by XRD: Comparison of a Rietveld and a reference intensity ratio (RIR) method and the importance of sample preparation. *Clay Miner.* **2000**, *35*, 291–302. [CrossRef]

21. Gualtieri, A.F. Accuracy of XRPD QPA using the combined Rietveld-RIR Method. *J. Appl. Crystallogr.* **2000**, *33*, 267–278. [CrossRef]

22. Rogkala, A.; Petrounias, P.; Tsikouras, B.; Hatzipanagiotou, K. New occurrence of pyroxenites in the Veria-Naousa ophiolite (north Greece): Implications on their origin and petrogenetic evolution. *Geosciences* **2017**, *7*, 92. [CrossRef]

23. Mercier, J.; Vergely, P.; Bebien, J. Les ophiolites helleniques "obductees" au Jurassique superieursont-elles les vestiges d' un ocean tethysienou d' une mermarginale perieuropeenne. *C. R. Somm. Soc. Geol. France* **1975**, *17*, 108–112.

24. Economou, M. A short note on the evolution of the Vermion ophiolite complex (Macedonia-Greece). *Ofioliti* **1983**, *8*, 333–338.

25. Michailidis, K.M. Zoned chromites with high Mn-contents in the Fe-Ni-Cr-laterite ore deposits from the Edessa area in Northern Greece. *Miner. Deposita* **1990**, *25*, 190–197. [CrossRef]

26. Economou-Eliopoulos, M. Apatite and Mn. Zn. Co-enriched chromite in Ni-laterites of northern Greece and their genetic significance. *J. Geochem. Explor.* **2003**, *80*, 41–54. [CrossRef]

27. Tsoupas, G.; Economou-Eliopoulos, M. High PGE contents and extremely abundant PGE-minerals hosted in chromitites from the Veria ophiolite complex. Northern Greece. *Ore Geol. Rev.* **2008**, *33*, 3–19. [CrossRef]

28. Saccani, E.; Photiades, A.; Santato, A.; Zeda, O. New evidence for supra-subduction zone ophiolites in the Vardar zone of northern Greece: Implications for the tectonomagmatic evolution of the Vardar oceanic basin. *Ofioliti* **2008**, *33*, 65–85.

29. Rogkala, A.; Petrounias, P.; Tsikouras, B.; Hatzipanagiotou, K. Petrogenetic significance of spinel from serpentinised peridotites from Veria-Naousa ophiolite. *Bull. Geol. Soc. Gr.* **2016**, *50*, 1999–2008.

30. Eleftheriadis, G.; Castorina, F.; Soldatos, T.; Masi, U. Geochemical and Sr-Nd isotopic evidence for the genesis of the Late Cainozoic Almopia volcanic rocks (Central Macedonia, Greece). *Mineral. Petrol.* **2003**, *78*, 21–36. [CrossRef]

31. Brunn, J.H. *Geological Map of Greece, Veroia Sheet, 1:50.000*; IGME: Athens, Greece, 1982.

32. *Part 1: Composition, Specifications and Conformity Criteria for Common Cements*; EN 197-1; European Standard: Warsaw, Poland, 2011.

33. *Resistance to Abrasion of Small-Size Coarse Aggregate by Use of the Los Angeles Machine*; ASTM C-131; American Society for Testing and Materials: Philadelphia, PA, USA, 1989.

34. *Standard Test Method for Unconfined Compressive Strength of Intact Rock Core Specimens*; ASTM D 2938-95; American Society for Testing and Materials: West Conshohocken, PA, USA, 2002.

35. *Part 3: Procedure and Terminology for Simplified Petrographic Description*; EN 932; European Standard: Warsaw, Poland, 1996.

36. *Methods for Sampling and Testing of Mineral Aggregates, Sands and Fillers, Part 1: Methods for Determination of Particle Size and Shape*; British Standard Institution: London, UK, 1975.

37. *Standard for Selecting Proportions for Normal, Heavyweight and Mass Concrete*; ACI-211.1-91; American Concrete Institute: Farmington Hills, MI, USA, 2002.

38. *Part 3: Testing Hardened Concrete. Compressive Strength of Test Specimens*; BS EN 12390; British Standard: London, UK, 2009.

39. *Standard Practice for Petrographic Examination of Hardened Concrete*; ASTM C856; American Society for Testing and Materials: West Conshohocken, PA, USA, 2017.

40. Rigopoulos, I.; Tsikouras, B.; Pomonis, P.; Hatzipanagiotou, K. Determination of the interrelations between the engineering parameters of construction aggregates from ophiolite complexes of Greece using factor analysis. *Constr. Build. Mater.* **2013**, *49*, 747–757. [CrossRef]

41. Barttli, B. The influence of geological factors on the mechanical properties of basic igneous rocks used as road surface aggregates. *Eng. Geol.* **1992**, *33*, 31–44. [CrossRef]

42. Smith, M.R.; Collis, L. *Aggregates: Sand, Gravel and Crushed Rock Aggregates for Construction Purposes*; Spec. Publ. 17; The Geological Society: London, UK, 2001.

43. Escartin, J.; Hirth, G.; Evans, B. Strength of slightly serpentinized peridotites: Implications for the tectonics of oceanic lithosphere. *Geology* **2001**, *29*, 1023–1026. [CrossRef]

44. Frost, B.R.; Beard, J.S. On silica activity and serpentinization. *J. Petrol.* **2007**, *48*, 1351–1368. [CrossRef]

45. Evans, B.W. Control of the products of serpentinization by the $Fe^{2+}Mg_{-1}$ exchange potential of olivine and orthopyroxene. *J. Petrol.* **2008**, *49*, 1873–1887. [CrossRef]

46. Jöreskog, K.G.; Klovan, J.E.; Reyment, R.A. *Geological Factor Analysis*; Elsevier: Amsterdam, The Netherlands, 1976.

47. Zoltai, T.; Stout, J.H. *Mineralogy Concepts and Principles*; Burgess Publishing Co.: Minneapolis, MN, USA, 1984.

48. Taylor, R.K.; Smith, T.J. The engineering geology of clay minerals; swelling, shrinking and mudrock breakdown. *Clay Miner.* **1986**, *21*, 235–260. [CrossRef]

49. Higgs, N.B. Preliminary studies of methylene blue adsorption as a method of evaluating degradable smectite-bearing concrete aggregate sands. *Cem. Concr. Res.* **1986**, *16*, 525–534. [CrossRef]

50. Farrokhpay, S.; Ndlovu, B.; Bradshaw, D. Behaviour of swelling clays versus non-swelling clays in flotation. *Miner. Eng.* **2016**, *96–97*, 59–66. [CrossRef]